Powder Technology 214 (2011) 194–199

Contents lists available at SciVerse ScienceDirect

Powder Technology

journal homepage: www.elsevier.com/locate/powtec

Cold compaction study of Armstrong Process® Ti–6Al–4V powders ☆

W. Chen [a], Y. Yamamoto [a,*], W.H. Peter [a], S.B. Gorti [a], A.S. Sabau [a], M.B. Clark [a], S.D. Nunn [a], J.O. Kiggans [a], C.A. Blue [a], J.C. Williams [b], B. Fuller [c], K. Akhtar [c]

[a] Materials Science and Technology Division, Oak Ridge National Laboratory, Oak Ridge, TN 37831, USA
[b] Department of Materials Science and Engineering, Ohio State University, Columbus, OH 43210, USA
[c] Cristal US, Inc./International Titanium Powder, Woodridge, IL 60157, USA

ARTICLE INFO

Article history:
Received 2 December 2010
Received in revised form 3 June 2011
Accepted 7 August 2011
Available online 16 August 2011

Keywords:
Titanium alloys
Die-pressing
Powder metallurgy
Armstrong process

ABSTRACT

The Armstrong Process® developed by Cristal US, Inc./International Titanium Powder, is an innovative, low-cost technology for producing Ti and Ti alloy powders in a one-step, continuous process. In this work, Armstrong Ti–6Al–4V powders were characterized and the cold compaction behavior of the powders were investigated in detail. As-received as well as milled powders were uniaxially die-pressed at designated pressures up to 690 MPa to form disk samples with different aspect ratios. Samples with high aspect ratio exhibited non-uniform density along the pressing axis and the density distribution was consistent with the result predicted by finite element analysis. The model developed from the linear regression analysis on the experimental density data can be used to predict density of compacts with different aspect ratios. In the studied pressure range, an empirical powder compaction equation was applied to linearize the green density — pressure relationship. Cold compaction parameters were obtained for the as-received and milled Armstrong Ti–6Al–4V powders.

© 2011 Elsevier B.V. All rights reserved.

1. Introduction

Titanium (Ti) and Ti alloys are attractive for industrial applications because of their low density, high specific strength and stiffness, adequate creep and fatigue strength, good corrosion resistance and adequate fracture toughness [1–3]. However, the high price of Ti has been a major stumbling block for its wide use in some areas, such as the automotive industry. Powder metallurgy (PM) offers a viable tool to produce near-net-shape components with little machining, thus reducing the manufacturing costs and increasing the material yield, commonly referred to as the "buy-to-fly ratio" in the aerospace sector.

The Press and sinter processing is a traditional PM method and has been used to make steel and copper based alloy parts for a wide range of applications. However, the high cost of Ti powder fabrication processes (i.e. the gas-atomization with low oxygen level) has limited the application for Ti PM parts. The Armstrong Process®, developed by Cristal US Inc./International Titanium Powder, Inc. (Woodridge, IL), is a novel, low-cost Ti powder fabrication process which produces high purity Ti and Ti-alloy powders in a one-step, continuous process [4–6], as illustrated in Fig. 1. In the process of producing Ti–6Al–4V alloy powder, metal chlorides vapor are injected into a flowing stream of liquid sodium (Na) to make the alloy powder directly. Since the Armstrong Process® has a potential to reduce the cost of Ti and Ti-alloy powders, it is expected that this process combined with the existing and developing PM technology will reduce final parts production cost by up to 50% [4]. Some preliminary research has been performed by the current authors on evaluating and optimizing the fabrication processes for near-net-shape components using Armstrong commercially pure titanium (CP-Ti) and Ti–6Al–4V (Ti-64) powders, such as die-pressing, cold isostatic pressing (CIP), hot isostatic pressing (HIP), and pneumatic isostatic forging (PIF) [7,8]. This paper describes more details on the die-pressing process of Armstrong Ti-64 powders. The green density — die pressure relationships have been discussed with different aspect ratios (thickness to diameter) and fitted with a powder compaction equation developed by Panelli [9], in order to clarify the effect of die-wall friction on the green density as a function of applied die-pressure. The density distribution in the as-pressed samples was also evaluated.

2. Materials and methods

Ti-64 powders were produced by the Armstrong Process®. Some powders were ball-milled using a polyethylene jar with ~13 mm diameter yttrium stabilized zirconia (ZrO_2) media in ethanol for 1 h and the resultant, minus 100 mesh (<140 μm) powders, were used for the current study. Powder chemistry was evaluated using inert gas fusion (ASTM E 1409–08, for oxygen) and combustion infrared detection (ASTM E 1941–04, for carbon). The morphology of the

☆ Notice: This manuscript has been authored by UT-Battelle, LLC, under Contract No. DE-AC05-00OR22725 with the U.S. Department of Energy. The United States Government retains and the publisher, by accepting the article for publication, acknowledges that the United States Government retains a non-exclusive, paid-up, irrevocable, world-wide license to publish or reproduce the published form of this manuscript, or allow others to do so, for United States Government purposes.

* Corresponding author. Tel.: +1 865 576 7095; fax: +1 865 574 4357.
E-mail address: yamamotoy@ornl.gov (Y. Yamamoto).

0032-5910/$ – see front matter © 2011 Elsevier B.V. All rights reserved.
doi:10.1016/j.powtec.2011.08.007

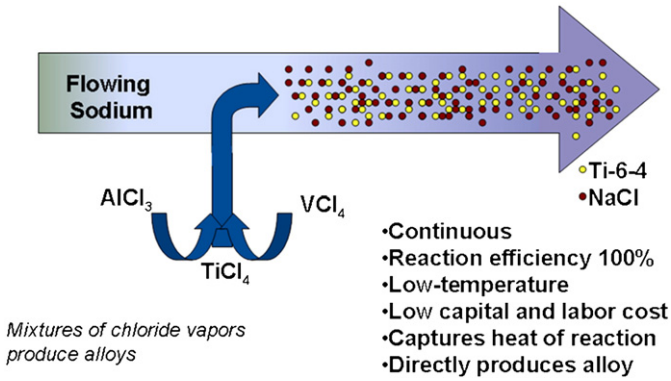

Fig. 1. The Armstrong direct alloy process for producing Ti–6Al–4V powder [6].

Armstrong Ti-64 powder was characterized using a JEOL-6500 (JEOL, Inc.) scanning electron microscope (SEM).

A steel die with an inner diameter of 1.27 cm (0.5 in.) was used for powder pressing at room temperature. The Ti-64 powders were uniaxially pressed (double-action) at several designated pressures: 17, 34, 69, 172, 345, and 690 MPa (2.5, 5, 10, 25, 50, and 100 ksi). Both as-received powders and milled powders were pressed. For the powders in the as-received condition, 2 g of powders were used for each sample. The milled powders were used to study the effect of aspect ratio on green density so the amount of powder used varied from 2.5 g to 10 g depending on the chosen aspect ratio studied. Disk samples with nominal aspect ratios (thickness to diameter) of 0.5, 1, and 2 were obtained at each pressure. For each combination of pressure and aspect ratio, four samples were made: The first sample was pressed and the peak pressure dwell time was less than 3 s (s); the second sample was kept at the designated pressure for 30 s; the third sample was kept at the designated pressure for 120 s; the forth sample was pressed using repeated pressure strikes without dwelling (3 times).

The density of the as-pressed samples was obtained by measuring the mass with a scale and the volume with dimensional measurement tools. Several as-pressed samples with higher aspect ratios were sectioned into 4 equal-thickness pieces and concentric rings. The density of each piece was calculated by measuring the mass and volume to evaluate the density distribution in the axial and radial directions.

3. Results and discussion

3.1. Powder characterization

Secondary electron-scanning electron microscopy (SE-SEM) photomicrographs of the Armstrong Ti-64 powder are illustrated in Fig. 2. The powder has an irregular coral like, dendritic morphology, with a dendrite size of approximately 2–5 μm, with a tap density of 6–8%. The size distribution of the Armstrong Ti-64 powder (milled for 1 h) is shown in Fig. 3. The milling process significantly reduced the powder size and increased the tap density to 30–32%. The chemical composition of the as-received Armstrong Ti-64 powder in weight percent was measured to be Al-5.95, V-3.82, O-0.16, N-0.13 and Ti-Balance.

3.2. Density–pressure relationships

Density–pressure curves have been widely used to study the compaction behavior of powders [10,11]. Fig. 4 shows a discontinuous

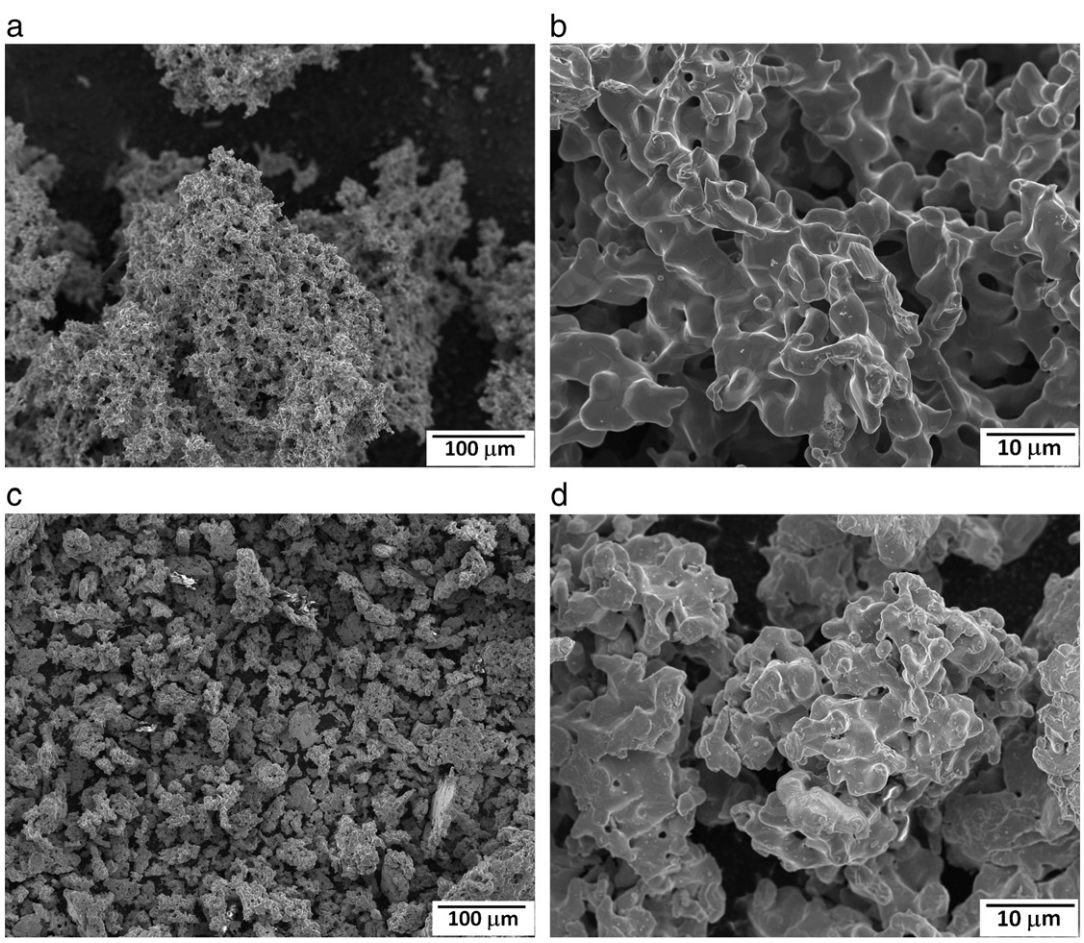

Fig. 2. SE SEM images of Armstrong Ti-64 powder. (a) and (b): as-received powder; (c) and (d): 1-h milled powder.

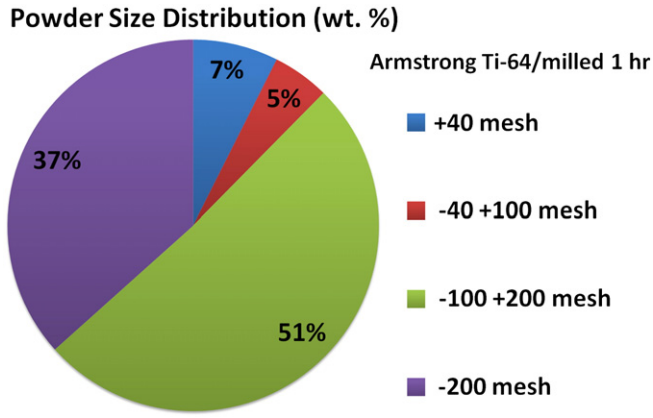

Fig. 3. Size distribution of 1-h milled Armstrong Ti-64 powder.

compaction curve obtained by die-pressing approximately 2 g of as-received Armstrong Ti-64 powder at designated pressures up to 690 MPa (100 ksi). Three samples were pressed at each pressure and the average value was used for plotting.

The green density increased monotonically with increasing pressure, but the slope of the curve decreased, indicating a lower compressibility at higher pressure in the range of this study.

The compaction of powders has been suggested to be a multi-stage process [12]. Fischmeister and Arzt [13] suggested a three-stage model for the densification process of spherical powders:

Stage I particle rearrangement, which occurs at the very beginning of compaction and does not contribute significantly to the densification of spherical powders;

Stage II particle plastic deformation, in which particles are flattened and brought closer to form additional contacts;

Stage III particle impinging, in which neighboring contacts on one particle impinge, making an increasing fraction of the volume harder to compress.

Poquillon et al. [14] studied the cold compaction behavior of a spongy iron powder which is quite similar in morphology to the Armstrong Ti-64 powder. Three deformation stages were clearly observed for the iron powder and particle interlocking was dominant and increased with compaction pressure. The current authors used an in-situ technique to observe the deformation of Armstrong commercially pure (CP) Ti powder [15], which has similar morphology to Armstrong Ti-64 powder. The powder compression test was performed using a screw-driven tensile stage placed inside an SEM. Powder agglomerates showed rotation (rearrangement) and fractured in the first two stages of compaction deformation. The corresponding stresses for these two stages were below 10 MPa. In the final stage of compression, the powders were squeezed and individual particles were brought closer to each other. The deformation process of Armstrong Ti-64 powders is expected to be the same as the Armstrong CP-Ti powder. The lowest pressure in the current study was 17 MPa (2.5 ksi), hence the compaction behavior described lies in stage III.

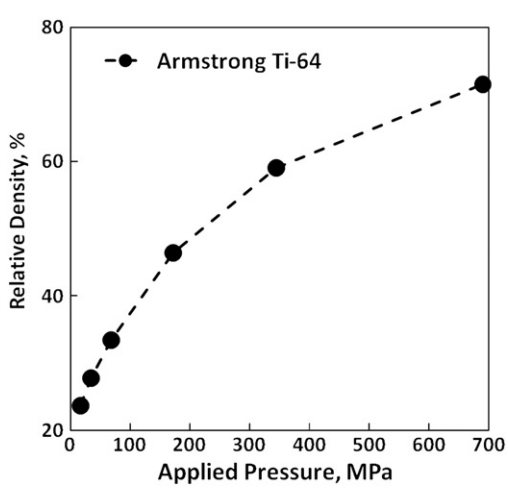

Fig. 4. Green density of the as-received Armstrong Ti-64 powders as a function of applied die-pressure plot.

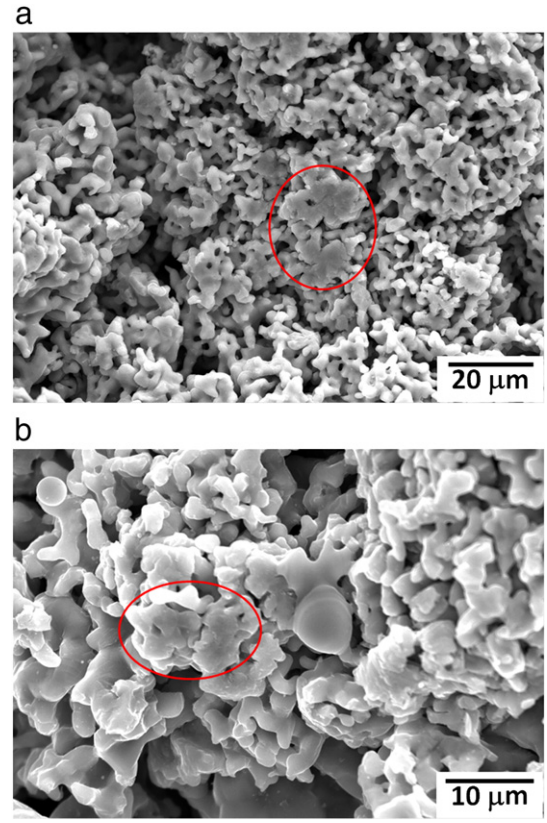

Fig. 5. SE SEM images of powder configuration in the (a) 172 MPa as-pressed sample, and (b) 345 MPa as-pressed sample. Notice that most Ti-64 particles are not deformed and heavily deformed particles are circled out.

Selected samples were intentionally broken in order to observe the open surface which preserved the configuration of deformed powders in the as-pressed condition. Fig. 5 illustrates the open surface of the samples pressed at 172 MPa (Fig. 5a) and 345 MPa (Fig. 5b). In most areas, the shape of individual Ti-64 particles is preserved without any deformation. Only a few heavily deformed particles are observed as shown in the circles in Fig. 5, which clearly indicates that local particle interlocking takes place due to the complicated dendritic shape of Armstrong Ti-64 particles. The particle interlocking results in the deformation of local portions, and then restricts further densification of the powder compacts. When two particles are pressed against each other, the material starts to yield when the local pressure becomes higher than the material yield strength (YS). As the particles yield, the contact area between particles increases, requiring higher pressures to continue deformation. According to Von Mises yield criterion, the material starts yielding when the local pressure reaches a value of approximately 1.1 times the material's yield strength (YS) [16]. The yield criterion

$$f = 3\sigma_y a \tag{1}$$

was adopted for analysis by Fischmeister and Arzt [13], in which f is the contact force, a is the contact area.

The room-temperature compressive YS of Ti-64 is 917 MPa [17], which is much higher than the die-pressure (172 and 345 MPa) experienced by the samples in Fig. 5. The contact pressure between most particles was not high enough to cause yielding of the Ti-64 particles. During the die-pressing process, the dendrite arms of the Armstrong Ti-64 powder were crushed and the interlocking between individual particles created more pronounced constraints. This type of geometrical hardening plays a role as important as the strain hardening of the material itself in the final stage of compaction process [13,18]. The extent of the variation of particle interlocking may have contributed to the porosity variation in the as-pressed Armstrong Ti samples [7].

Pressure dwell time proved to be an effective way of increasing the green density of Armstrong CP-Ti [7]. The average green density (pressed at 690 MPa) increased from 88.4% to 91.8% (30 s dwell time) and 92.2% (120 s dwell time). The density increase was due to the plastic deformation of CP-Ti powders since the compressive YS of CP-Ti is 520 MPa at RT (ASTM Grade 4) [1]. However, pressure dwelling had little effect on the density of Armstrong Ti-64 (Fig. 6) in the pressure range studied, which would be due to its much higher YS (917 MPa at RT). Repeated pressure strikes also did not increase the green density of Armstrong Ti-64, possibly due to the same reason.

3.3. Green density distribution

It is well known that the friction between powder and die-wall creates stress gradients within the powder bed, leading to density fluctuations in the green components, and this non-uniform green density will cause shape distortion after sintering [10]. The green density variation increases with the sample aspect ratio. A computational model was developed and implemented in the commercial finite element program ABAQUS™ to simulate the cold pressing process. The green density distribution of Armstrong powders die-pressed at 517 MPa was predicted as shown in Fig. 7. The details of the computational model can be found elsewhere [18,19]. For the thin samples with an aspect ratio of 0.8 (Fig. 7b), the density was quite uniform except in a very limited area near the surface. For the thick sample with an aspect ratio of 3.5 (Fig. 7c), the density variation was significant and the density gradient became higher. The highest and lowest densities were found at the top and center of the outer circumferences respectively, with the density decreasing gradually from top to center. Although the simulation result was based on Armstrong CP-Ti powders, it is expected that Armstrong Ti-64 powder will have a similar density distribution.

The green density distribution was also evaluated experimentally. The overall green density was 57.5% and 63.3% for the Armstrong Ti-64 powders pressed at 345 MPa and 517 MPa, with aspect ratio 2, respectively. The samples were sectioned into 4 pieces and the density

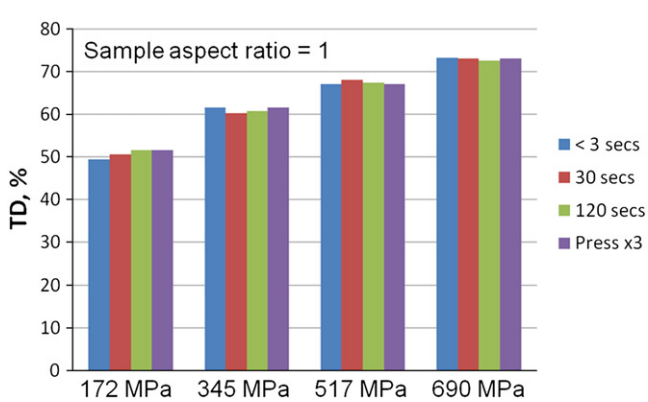

Fig. 6. The effect of dwell time and repeated pressure strikes on green density of Armstrong Ti-64 powders.

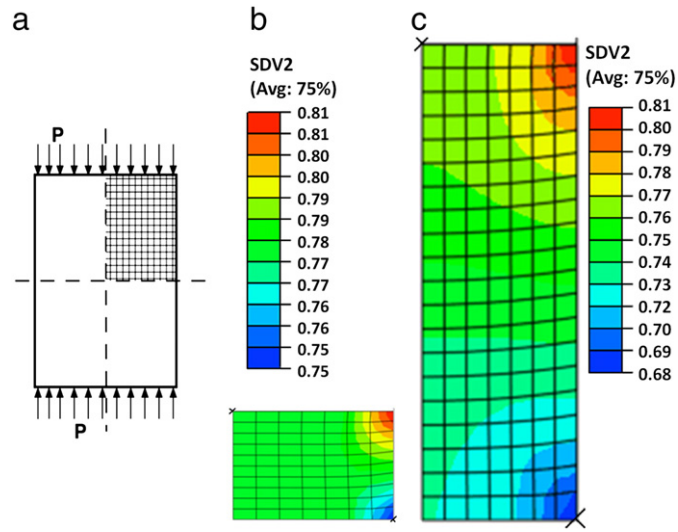

Fig. 7. FEM analysis of green density distribution in Armstrong CP-Ti samples (pressed at 517 MPa) [19]: (a) mesh for compaction of cylinders, (b) computed density distribution in a sample with aspect ratio equals 0.8, and (c) computed density distribution in a sample with aspect ratio equals 3.5. Deformed meshes are shown in (b) and (c).

of each piece was measured, as shown in Fig. 8a. It is clear that the density of the middle two pieces is lower than that from top to bottom, and a higher pressure led to a larger density difference. For the sample pressed at 345 MPa, the average density difference between the middle two pieces and the top plus bottom pieces was 5.5%; while the sample pressed at 517 MPa exhibited 6.3% difference. For a given aspect ratio, the overall, maximum and minimum densities in each sample increased with the applied die-pressure. This is consistent with the findings by Briscoe and Rough [20]. The axial density variation is in agreement with the simulation result in Fig. 8. In addition, two samples were sectioned into concentric rings to evaluate the radial density variation (Fig. 8b). The density in the radial

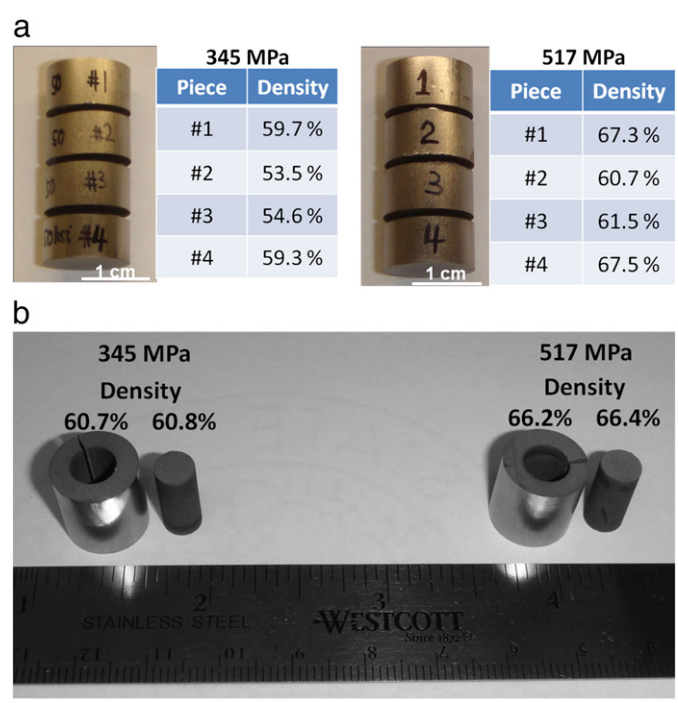

345 MPa Piece	Density
#1	59.7 %
#2	53.5 %
#3	54.6 %
#4	59.3 %

517 MPa Piece	Density
#1	67.3 %
#2	60.7 %
#3	61.5 %
#4	67.5 %

Fig. 8. Green density distribution in Armstrong Ti-64 samples pressed at 345 MPa and 517 MPa. (a) axial density of samples with aspect ratio 2, and (b) radial density of samples with aspect ratio 1.

direction was uniform. The result is expected since the reduction of the powder bed height during the pressing process is physically uniform along the radial direction. Lubricants have been widely used to reduce die-wall friction [10] and hence reduce the green density variation [20]. However, this may not be practical for Ti powders for certain market application since the mechanical properties of Ti are extremely sensitive to contamination, especially oxygen, nitrogen, hydrogen, and carbon.

3.4. Density — aspect ratio analysis

Fig. 9a illustrates the effect of aspect ratio on green density at six different applied die pressures and the detailed density data are included in Table 1 (Due to the physical limit of the die, a sample with an aspect ratio of 2 is not obtainable at 690 MPa). In Table 1, |a| value, is the slope of the linear curve and an indication of the extent of die-wall friction. If there is no friction, |a| should be zero. The Y-intercept (b value) is the relative density when the aspect ratio equals zero and can be used to estimate the green density when there is no friction. Fig. 9a can also be used to estimate the green density of samples with different aspect ratios as a function of compaction pressures. Die-wall friction is related to the radial wall stress transmitted by powders through axial stress, so it is a material-dependent value and difficult to measure experimentally. Janssen–Walker differential slice analysis [21] has been used to predict the value of the mean axial stress across a horizontal plane at a certain height [20,22]. In those studies, only an estimated value of stress transmission coefficient was used for density prediction. In addition, experimental data showed that the locally induced normal stress significantly changed the friction coefficient between powder and die-wall [23].

Fig. 9a shows that at 34 MPa, the density was almost identical regardless of aspect ratios, indicating that the die-wall friction was negligible at this stress level. Thus the slope of the linear curve fitting (|a| value) was only 0.2. As the applied die pressure increased, the density of samples decreased with increasing aspect ratios due to higher frictional force between the powder and the die-wall. The |a| value increased monotonically and reached 2.9 at 690 MPa. Fig. 9b shows the |a| value as a function of die-pressure. At low die-pressure, the |a| value increased rapidly, indicating a fast increase of die-wall friction and the percentage of stress transferred from punch to powder bed decreased significantly. However, as the die-pressure increased, the rate of friction increment became mild. It is likely that the increased die-pressure was dissipated by the plastic deformation of powders and only a small portion was transferred to the die-wall.

3.5. Powder pressing linear regression analysis

There are 4 widely used empirical compaction equations which have been developed by Heckel [24], Kawakita [25], Ge [26], and Panelli [9]. A critical review of these equations [27] showed that the Panelli equation best represents the density–pressure relationship for the 22 different powders studied in that investigation. The density–pressure data for the Armstrong Ti-64 powders were analyzed using the Panelli equation:

$$ln\left(\frac{1}{1-D}\right) = A\sqrt{P} + B \quad (2)$$

in which D is the relative density of the compacted material and P is the applied die pressure. A is a constant which represents the compressibility (powder's ability to densify by plastic deformation).

$$B = ln\left(\frac{1}{1-D_0}\right) \quad (3)$$

B is the Y-intercept, where D_0 represents the loose powder density (tap density).

Fig. 10a shows the density–pressure data for the as-received Armstrong Ti-64 powders fitted to Eq. (2). Fig. 10b shows the curve fitting for the milled powder pressed to 3 different aspect ratios. The curve fitting parameters are also listed in Table 2. The linear correlation coefficient was greater than 0.99 in all cases, indicating a good agreement between Eq. (2) and the experimental data. For the milled powder, A decreased from 0.040 to 0.034 as the aspect ratio increased from 0.5 to 2. The increased die-wall friction due to the higher aspect ratio reduced the pressure transferred to the powder bed and caused the decrease of apparent compressibility of the Armstrong Ti-64 powder. The three curves converged at the lower pressure end, indicating the decrease of friction at a lower pressure. The predicted tap density (D_0) was 5.3% for the as-received powder and 17.9–20.6% for the milled powder. The values are all lower than the experimentally measured tap density (6–8% for as-received powder and 30–32% for the milled powder). The discrepancy indicates the limitation of the Panelli equation at low pressures (Stages I and II) so extrapolation into this area is not accurate due to the different densification mechanisms. However, the density prediction within the studied pressure range (Stage III) shows good agreement. The A value of the as-received powder is larger than the milled powder, indicating its

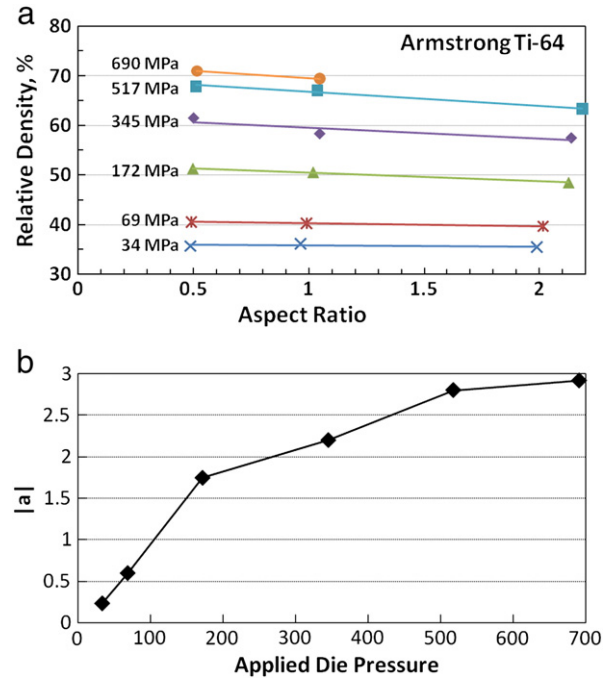

Fig. 9. (a) Green density versus aspect ratio plot for the Armstrong Ti-64 samples pressed at 6 different pressures, and (b) the change of |a| value (line slope) versus the die-pressure.

Table 1
Green density data and linear regression parameters for Armstrong Ti-64 samples.

Pressure, MPa	Relative density,%			Linear regression	
	Nominal sample aspect ratio			Y = aX + b	
	0.5	1	2	|a|	b
34	35.7	36.2	35.5	0.2	36.1
69	40.6	40.3	39.7	0.6	40.9
172	51.3	50.6	48.5	1.8	52.3
345	61.5	58.3	57.5	2.2	61.8
517	67.9	67.1	63.3	2.8	69.6
690	71.0	69.4	N/A	2.9	72.5

N/A: Not available.

Table 2
Density–pressure liner curve fitting parameters for the Armstrong Ti-64 samples.

Powder condition	Aspect ratio	Linear curve fitting parameters			
		A	B	R^2	D_0
As-received	N/A	0.045	0.055	0.9954	5.3%
Milled/1 h	0.5	0.040	0.198	0.9979	17.9%
	1	0.038	0.214	0.9919	19.3%
	2	0.034	0.231	0.9989	20.6%

N/A: Not available.

less compressibility. This could be due to the complicated morphology of the as-received powder, which increased the deformation resistance.

4. Conclusions

The low-cost Ti-64 powder produced by the Armstrong Process was characterized. The powder has an irregular coral like, dendritic morphology, with a dendrite size of approximately 2–5 μm. The die-pressing behavior of Armstrong Ti-64 powders was studied in the case of disk shape compacts with 3 different aspect ratios, namely 0.5, 1, and 2. The density distribution in the as-pressed samples was evaluated experimentally and is consistent with the simulation result by finite element analysis. The density in the middle section along the axial direction was lower and higher pressure led to larger density variation.

The die-wall friction increased with the applied die-pressure causing a change in the slope of the linear regression model generated from the density data. The overall density of Armstrong Ti-64 powder compacts with different aspect ratios at six designated pressures was predicted. In the studied die-pressure range, an empirical powder compaction equation: $ln(1/(1-D)) = A\sqrt{P} + B$, linearized the relationship between the green density (D) and die-pressure (P) very well for both the as-received and milled Armstrong Ti-64 powders. The predicted tap density D_0 is lower than the experimental value, indicating the limitation of the Panelli equation at very low pressure. This study will provide guidance for the future development of PM processing for the near-net-shape manufacturing of Ti components using Armstrong Ti-64 powders.

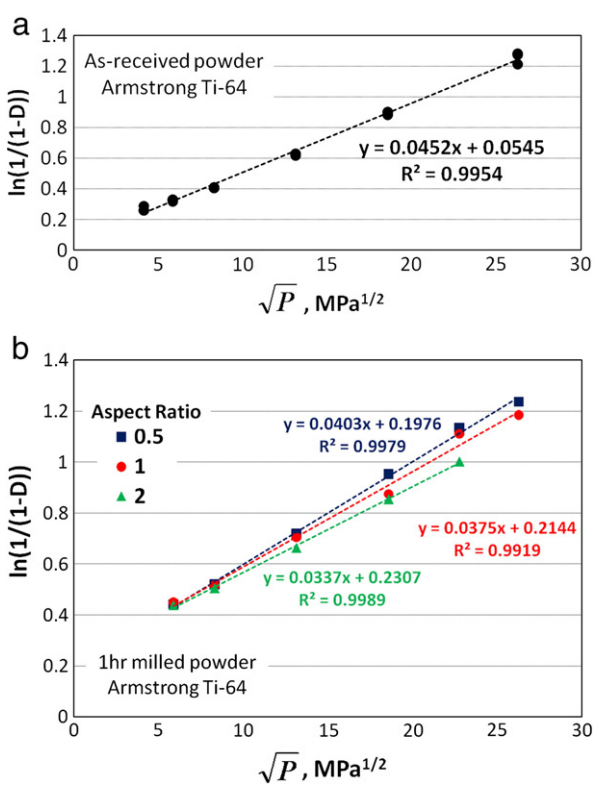

Fig. 10. Green density versus die-pressure fitted to the Panelli equation for the Armstrong Ti-64 (a) as-received powders, and (b) 1-h milled powders.

Acknowledgments

This research is sponsored by the U.S. Department of Energy, Office of Energy Efficiency and Renewable Energy (EERE) Industrial Technologies Program, under contract DE-AC05-00OR22725 with UT-Battelle, LLC. Additional funding and collaboration with the SHaRE User Facility (microscopy) at ORNL is also acknowledged.

References

[1] R. Boyer, G. Welsch, E.W. Collings, Materials Properties Handbook: Titanium Alloys, ASM International, Materials Park, OH, 1994.
[2] G. Lutjering, J.C. Williams, Titanium, Springer-Verlag, Berlin Heidelberg, 2007.
[3] C. Leyens, M. Peters, Titanium and Titanium Alloys: Fundamentals and Applications, WILEY-VCH Verlag GmbH & Co, KGaA, Weinheim, 2003.
[4] G. Crowley, Adv. Mater. Process. 161 (2003) 25–27.
[5] R. Anderson, A. Benish, L. Jacobsen, W. Ernst, D. Kogut, Development status of the Armstrong Process for production of low cost titanium powder, 16th Annual AeroMat Conference, Orlando, FL, June 6–9, 2005.
[6] F.H. Froes, M.N. Gungor, M.A. Imam, Cost-affordable titanium: the component fabrication perspective, JOM 59 (2007) 28–31.
[7] Y. Yamamoto, J.O. Kiggans, M.B. Clark, S.D. Nunn, A.S. Sabau, W.H. Peter, Consolidation process in near net shape manufacturing of Armstrong CP-Ti/Ti–6Al–4V powders, Key Eng. Mater. 436 (2010) 103–111.
[8] Y. Yamamoto, W.H. Peter, A.S. Sabau, S.B. Gorti, J.O. Kiggans, S.D. Nunn, M.B. Clark, C.A. Blue, J.E. Barnes, C. Henry, J.A. Capone, M. Paliwal, B. Fuller, K. Akhtar, Advances in Powder Metallurgy & Particulate Materials — 2010, in: M. Bulger, B. Stebick (Eds.), Metal Powder Industries Federation, Princeton, NJ, 2010, pp. 24–27, part 3.
[9] R. Panelli, F. Ambrozio Filho, A compacting equation and its use to describe the powder consolidation behavior, Powder Metall. 41 (1998) 131–133.
[10] R.M. German, Powder Metallurgy and Particulate Materials Processing, Metal Powder Industries Federation, Princeton, NJ, 2005.
[11] L.F. Pease, W.G. West, Fundamentals of Powder Metallurgy, Metal Powder Industries Federation, Princeton, NJ, 2002.
[12] P.J. James, Fundamental aspects of the consolidation of powders, Powder Metall. Int. 4 (1972) 82–85.
[13] H.F. Fischmeister, E. Arzt, Densification of powders by particle deformation, Powder Metall. 26 (1983) 82–88.
[14] D. Poquillon, J. Lemaitre, V. Baco-Carles, Ph. Tailhades, J. Lacaze, Cold compaction of iron powders-relations between powder morphology and mechanical properties Part I: powder preparation and compaction, Powder Technol. 126 (2002) 65–74.
[15] W. Chen, Y. Yamamoto, W.H. Peter, Investigation of pressing and sintering processes of CP-Ti powder made by Armstrong Process, Key Eng. Mater. 436 (2010) 123–130.
[16] D. Tabor, A simple theory of static and dynamic hardness, Proc. R. Soc. A 192 (1948) 247–274.
[17] R. Boyer, G. Welsch, E.W. Collings, Materials Properties Handbook: Titanium Alloys, ASM International, Materials Park, OH, 1994, p. 517.
[18] A.S. Sabau, J.O. Kiggans, W.H. Peter, D.L. Erdman III, Y. Wang, M.B. Clark, Material properties for the simulation of cold pressing of Armstrong CP-Ti powders, in: M. Bulger, B. Stebick (Eds.), Advances in Powder Metallurgy & Particulate Materials — 2010, Metal Powder Industries Federation, Princeton, NJ, 2010, pp. 1–10.
[19] A.S. Sabau, S.B. Gorti, W.H. Peter, Y. Yamamoto, Process simulation of cold pressing of Armstrong CP-Ti powders, in: M. Bulger, B. Stebick (Eds.), Advances in Powder Metallurgy & Particulate Materials — 2010, Metal Powder Industries Federation, Princeton, NJ, 2010, pp. 70–83.
[20] B.J. Briscoe, S.L. Rough, The effects of wall friction in powder compaction, Colloids Surfaces A 137 (1998) 103–116.
[21] R.M. Nedderman, The theoretical prediction of stress distributions in hoppers, Trans. Inst. Chem. Eng. 60 (1982) 259–275.
[22] N. Ozkan, B.J. Briscoe, Prediction of overall shape of sintered alumina compacts, J. Eur. Ceram. Soc. 14 (1994) 143–151.
[23] B.J. Briscoe, M.S.D. Fernando, A.C. Smith, The role of interfacial friction in the compaction of maize, in: B.J. Briscoe, M.J. Adams (Eds.), Tribology, Particulate Technology, Hilger, Bristol, 1987, pp. 220–233.
[24] R.W. Heckel, Density pressure relationship in powder compaction, Trans. Metall. Soc. AIME 221 (1961) 671–675.
[25] K. Kawakita, K. Ludde, Some considerations on powder compression equations, Powder Technol. 4 (1971) 61–68.
[26] R. Ge, A new equation for powder compaction, Powder Metall. Sci. Technol. 6 (1995) 20–24.
[27] R. Panelli, F.A. Filho, A study of a new phenomenological compacting equation, Powder Technol. 114 (2001) 255–261.